Original Research

Microbial electrosynthesis of acetate from CO_2 in three-chamber cells with gas diffusion biocathode under moderate saline conditions

Paolo Dessì [a, b, *], Claribel Buenaño-Vargas [c], Santiago Martínez-Sosa [a], Simon Mills [c], Anna Trego [c], Umer Z. Ijaz [d], Deepak Pant [e], Sebastià Puig [b], Vincent O'Flaherty [c], Pau Farràs [a]

[a] School of Biological and Chemical Sciences and Energy Research Centre, Ryan Institute, University of Galway, University Road, H91 CF50, Galway, Ireland
[b] LEQUiA, Institute of the Environment, University of Girona, Carrer Maria Aurèlia Capmany 69, E-17003, Girona, Spain
[c] Microbiology Department, School of Natural Sciences, University of Galway, University Road, H91 TK33, Galway, Ireland
[d] Infrastructure and Environment Research Division, School of Engineering, University of Glasgow, Glasgow, United Kingdom
[e] Separation and Conversion Technology, Flemish Institute for Technological Research (VITO), Boeretang 200, 2400, Mol, Belgium

ABSTRACT

The industrial adoption of microbial electrosynthesis (MES) is hindered by high overpotentials deriving from low electrolyte conductivity and inefficient cell designs. In this study, a mixed microbial consortium originating from an anaerobic digester operated under saline conditions (~13 g L^{-1} NaCl) was adapted for acetate production from bicarbonate in galvanostatic (0.25 mA cm^{-2}) H-type cells at 5, 10, 15, or 20 g L^{-1} NaCl concentration. The acetogenic communities were successfully enriched only at 5 and 10 g L^{-1} NaCl, revealing an inhibitory threshold of about 6 g L^{-1} Na^+. The enriched planktonic communities were then used as inoculum for 3D printed, three-chamber cells equipped with a gas diffusion biocathode. The cells were fed with CO_2 gas and operated galvanostatically (0.25 or 1.00 mA cm^{-2}). The highest production rate of 55.4 g m^{-2} d^{-1} (0.89 g L^{-1} d^{-1}), with 82.4% Coulombic efficiency, was obtained at 5 g L^{-1} NaCl concentration and 1 mA cm^{-2} applied current, achieving an average acetate production of 44.7 kg MWh^{-1}. Scanning electron microscopy and 16S rRNA sequencing analysis confirmed the formation of a cathodic biofilm dominated by *Acetobacterium* sp. Finally, three 3D printed cells were hydraulically connected in series to simulate an MES stack, achieving three-fold production rates than with the single cell at 0.25 mA cm^{-2}. This confirms that three-chamber MES cells are an efficient and scalable technology for CO_2 bio-electro recycling to acetate and that moderate saline conditions (5 g L^{-1} NaCl) can help reduce their power demand while preserving the activity of acetogens.
© 2023 The Authors. Published by Elsevier B.V. on behalf of Chinese Society for Environmental Sciences, Harbin Institute of Technology, Chinese Research Academy of Environmental Sciences. This is an open access article under the CC BY-NC-ND license (http://creativecommons.org/licenses/by-nc-nd/4.0/).

1. Introduction

Microbial electrosynthesis (MES) is an emerging electrochemical process that exploits microbial metabolism to reduce CO_2 to green chemicals [1]. In MES, specific microorganisms — electrotrophs — have been indicated to catalyse CO_2 reduction to multicarbon organic molecules and H^+ reduction to H_2 by directly uptaking electrons from the cathode electrode [2]. When mixed consortia of anaerobic microorganisms are used as inoculum, the community often evolves into a synergy between H_2-producing electrotrophs (e.g., *Desulfovibrio* sp.) and acetogens (e.g., *Acetobacterium* and *Clostridium* sp.) that reduce CO_2 using H_2 as electron donor through the Wood-Ljungdahl pathway (WLP) [3,4]. Microorganisms act as cheap, resilient, and self-regenerating catalysts capable of targeting specific products with high selectivity and, unlike metal-based catalysts, can be adapted to treat industrial flue gases with impurities [5]. However, the establishment of MES is still hindered by the current density, which remains 1−2 orders of magnitude lower than state-of-art electrolysers, and by the high cell voltages often deriving from sub-optimised cell design (mainly H-type cells) used in MES research [6].

Designing modular, scalable, electrically efficient cells is imperative to bring MES towards industrial application. Thus,

* Corresponding author. LEQUiA, Institute of the Environment, University of Girona, Carrer Maria Aurèlia Capmany 69, E-17003, Girona, Spain.
E-mail address: paolo.dessi@udg.edu (P. Dessì).

research and development efforts are progressively directed toward innovative MES cell configurations targeting industrially significant production rates [7]. For lab-scale experiments, 3D printing techniques can be used to design and realize innovative cell configurations at relatively low cost, fabricate custom electrodes [8] and even synthetic biofilms with embedded microorganisms [9]. Scalable set-ups should be achieved using inexpensive materials since large electrode surfaces will be required in full-scale MES installations due to the low current densities achievable with biocatalysts, theoretically limited to 50 mA cm^{-2} [10]. The investigated approaches to increase production rates include modified cathodes with high surface area, conductivity and hydrophobicity or specific cell design aimed at promoting biofilm adhesion and mass transfer between CO_2 gas, microorganisms, and electrolyte [11]. Among the proposed configurations, three-chamber cells equipped with a gas diffusion electrode (GDE) are an easily scalable technology that can promote mass transfer by overcoming the limitation of CO_2 solubility faced by aqueous-phase systems [12]. GDEs combine a polymeric layer for gas diffusion to a conductive layer acting as support for the development of the cathodic biofilm, which is exposed on-site to both substrates and reducing equivalents, limiting gas escape through the liquid electrolyte. This results in higher CO_2 conversion rates than submerged systems [13].

Besides inefficient reactor design, the electric efficiency of MES cells is often low due to the use of microbial-compatible, low-conductivity electrolytes (typically around 10 mS cm^{-1}), which cause high ohmic drop and, consequently, high cell voltages [6]. Using electrolytes with higher conductivity will result in substantial energy savings as long as the productivity of bacteria is not compromised. NaCl-based electrolytes could be used as a cost-efficient, strong electrolyte exhibiting high ionic conductivity [14], but their use in MES systems will require specific halotolerant/halophilic species that can thrive under saline conditions [15]. Nevertheless, acetogens have a highly diverse ecological niche, with representative species in different saline environments [16]. In some members of this group, such as *Acetobacterium woodii*, the reaction for growth and acetate formation from CO_2 and H_2 is strictly Na$^+$-dependent since it is driven by a chemiosmotic mechanism exploiting Na$^+$ gradients in the acetyl-CoA pathway [17]. Moreover, NaCl stress induces biofilm formation in acetogenic organisms such as *Clostridium ljungdahlii*, which is desirable in MES cells [18].

Despite the possible advantages, little information is available about the Na$^+$ tolerance threshold of these non-halophilic acetogens, particularly when combined with other common stressors typical of MES (including ion migration, oxygen intrusion, and acidic conditions). Alqahtani et al. [19,20] provided the first proof of concept on using microorganisms from saline habitats for CO_2 reduction in MES cells, demonstrating acetogenesis at up to 25% total salinity (above 200 mS cm^{-1} conductivity). However, acetate production was low (in the mg order) and unstable, with current densities mostly below 0.15 mA cm^{-2}. Zhang et al. [21] achieved a stable acetate production of 3.5 g m^{-2} d^{-1} at 35 g L^{-1} (3.5%) salinity after lowering the hardness of the catholyte by decreasing the Mg and Ca concentrations. The production rate was further increased to 9 g m^{-2} d^{-1} by implementing a three-chamber cell to avoid chloride oxidation at the anode. However, the system was only tested at a low current density of 0.156 mA cm^{-2}, with a coulombic efficiency not exceeding 35%, and without a substantial decrease of the cell voltage, which remained at 2.45 V. Thus, milder salinity conditions can represent a trade-off between microbial and electric efficiency to achieve the highest product synthesis per unit of electric power invested.

In this study, an inoculum previously acclimated for anaerobic digestion under saline conditions, i.e., ~13 g L^{-1} (1.3%) NaCl, was evaluated for acetate production in H-type MES cells fed with electrolytes containing 5, 10, 15, or 20 g L^{-1} NaCl. The best performing microbial consortia were then used as inoculum for 3D printed three-chamber cells operated galvanostatically and equipped with a GDE, operated at different current densities to achieve the highest acetate production rate from CO_2 as the sole carbon source. Moreover, three cells were hydraulically connected in series to simulate a MES cell stack and evaluate its overall performance compared to the single cells.

2. Materials and methods

2.1. Experiment set-up

2.1.1. H-type cell set-up

The H-type cells were previously described by Isipato et al. [22]. Briefly, they consisted of two glass chambers of 150 mL working volume, each separated by a Nafion 117 proton exchange membrane (8.5 cm^2, Fuel Cell Store, USA). The cathode chamber was connected to a gas bag (1 L), whereas the anode chamber was open to avoid the accumulation of oxygen in the headspace. The cells were equipped with a carbon cloth cathode (Panex 30 Fabric PW06, Fuel Cell Store, USA) and a Pt–Ti mesh anode (Goodfellow, UK) with a projected surface of 12 and 4 cm^2, respectively, at about 10 cm distance from each other. The cells were placed over a stirring plate (Cole-Parmer, US) to continuously mix the catholyte, connected to a potentiostat (Autolab M204, Metrohm, Switzerland) in a two-electrode configuration and operated under ambient conditions (18–24 °C).

2.1.2. Three-chamber cell set-up

Bespoke three-chamber cells (Fig. 1), with an approximate volume of 200 mL per chamber, were designed and 3D printed in UV-cured resin material (3D Technology Ltd, Ireland). A blueprint of the cell frames is available in Fig. S1 in the Supplementary material. A VITO-Core® GDE [23] with a projected surface of 64 cm^2 was used as the cathode, and Pt–Ti mesh (4 cm^2) was the anode. The two electrodes were separated by Nafion 117 membrane (64 cm^2). An Ag/AgCl reference electrode (Alvatek, UK) was added to the cathode chamber at an approximate distance of 1 cm from the GDE. Recirculation lines consisting of glass bottles and peristaltic pumps (Verder Vantage 300, UK) were installed in both the cathodic and anodic chambers, resulting in a total working volume of 400 mL per chamber. The gas feeding lines consisted of a pure CO_2 gas cylinder connected to a gas flow controller (EL-Flow base, Bronkhorst, The Netherlands) and the gas diffusion chamber of the cells through a nylon pipeline. Both the cathode and anode recirculation bottles were open to avoid overpressure from gas accumulation, but the cathode was protected from oxygen intrusion from the atmosphere through one-way valves (Fig. 1). The cell was connected to the potentiostat in a three-electrode configuration.

2.2. Inoculum, anolyte and catholyte

The inoculum was collected from a lab-scale anaerobic digester producing methane (CH$_4$) from saline (~13 g L^{-1} NaCl) synthetic wastewater containing acetate, glucose, and tryptone for over 500 days. The original inoculum was anaerobic digester sludge from a dairy processing industry (Carbery, Ireland). The anolyte contained (in g L^{-1}): KH$_2$PO$_4$ (0.33), K$_2$HPO$_4$ (0.45), NH$_4$Cl (1.0), KCl (0.1), MgSO$_4$•7H$_2$O (0.2), NaHCO$_3$ (4), and NaCl at different concentrations (5, 10, 15, or 20). In addition to those chemicals, the catholyte contained a mix of vitamins (1 mL L^{-1}) and trace metals (10 mL L^{-1}) (DSMZ medium 144). Sodium 2-bromoethanesulphonate (Na-BES, 1 g L^{-1}) was added to the catholyte at the beginning of each reactor
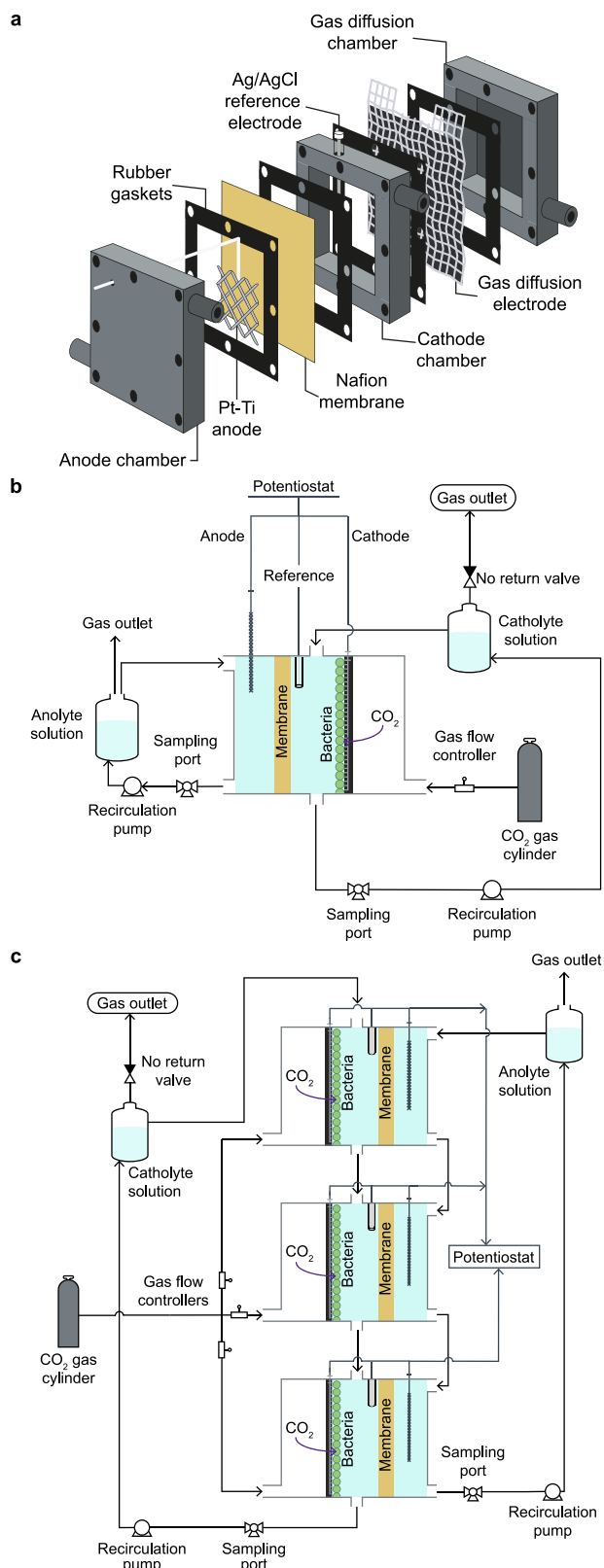
Fig. 1. a, Three-chamber cell design. **b−c**, Experimental design for a single three-chamber cell (**b**) and a stack of three cells (**c**).

run to prevent methanogenesis. The initial pH was set to 6 in the H-type cells, whereas it was set to 7 in the three-chamber cells to counteract the acidification caused by continuous CO_2 sparging.

2.3. MES cell operation and sampling

All single cell experiments were performed in duplicate. H-type cells were operated galvanostatically at an applied current of 3 mA (0.25 mA cm^{-2}) in a fed-batch mode for three consecutive cycles for a total of 40 days. At the end of each cycle, 10% (i.e., 15 mL) of fresh catholyte containing 40 g L^{-1} $NaHCO_3$ was supplied to restore the initial concentration of 4 g L^{-1}. Samples of both catholyte and anolyte were collected thrice per week. The pH, which showed a rising trend due to electrochemical OH^- generation at the cathode, was adjusted back to 6.0 (±0.1) at least weekly, or any time pH 9 was exceeded, by dosing 3 M HCl.

Three-chamber cells were operated for a total of 32−42 days under galvanostatic mode at an applied current of either 16 mA (0.25 mA cm^{-2}) or 64 mA (1.00 mA cm^{-2}). CO_2 gas was continuously supplied through the GDE at a constant rate of 2 mL min^{-1}. Both catholyte and anolyte were continuously recirculated at a flow rate of 25 mL min^{-1}. Liquid samples were collected thrice per week, excluding periods of high-rate production in which samples were collected daily. Gas samples were collected on each sampling day by connecting a gas bag to the cathode outlet for 2 h.

The stack consisted of 3x three-chamber cells hydraulically connected in series, resulting in a recirculation loop in which the outlet of a cell was connected to the inlet of the next cell (Fig. 1). Initially, the autotrophic community was enriched in a single cell containing 400 mL catholyte and anolyte with 5 g L^{-1} NaCl, as done in the previous experiment. After approximately 30 days, fresh catholyte and anolyte were added (up to a total volume of 900 mL each), and the valves between the three cells were opened to let the microorganisms colonise the other two cells. Both CO_2 (5 mL min^{-1} flow rate) and current (either 0.25 or 1.00 mA cm^{-2}) were independently supplied to the three cells. With respect to the single-cell experiments, a higher CO_2 flow rate was necessary to counteract oxygen intrusion through the three membranes, thereby maintaining anaerobic conditions.

2.4. SEM imaging and microbiological analysis

Scanning electrode microscope (SEM) analysis was performed as in Isipato et al. [22]. Briefly, cathodic samples were fixed using a glutaraldehyde and paraformaldehyde (2% each) solution in 0.1 M sodium cacodylate buffer, dried in increasing (30−100%) ethanol concentration, gold coated and imaged (SEM Hitachi S4700) at 15 kV and 50 μA. Samples of the cathodic communities were collected at the end of each experiment for microbial community analysis. For the H-type cells, the whole cathode electrode was gently removed and submerged in a Falcon tube containing 12 mL sterile anolyte solution with the same NaCl concentration present in the cell to avoid osmotic stress on the microorganisms. A similar approach was used for the GDE, which was submerged in a sterile glass container in 300−400 mL anolyte. The cathodic biofilm was detached by 5 min sonication (QR Kerry, Ireland), vigorous shaking and/or vortex (for the carbon cloth only). The GDE community was concentrated to a total of 12 mL by consecutive centrifugation (Eppendorf, Germany) at 7830 rpm in 50 mL Falcon tubes. The samples were then transferred in six replicate pre-weighted 2 mL Eppendorf tubes and centrifuged for 10 min at 10000 rpm (Legend Micro 17, Thermo Scientific). After discarding the supernatant, the pellets were weighted, snap-frozen in liquid nitrogen and stored at −80 °C for analysis.

DNA was extracted in triplicates from approximately 20−50 mg

of wet biomass. Before the extraction, samples were washed with 1 volume of PBS (1x), shaken at 300 rpm for 7 min, and pelleted by centrifugation at 12000g for 5 min. After discarding the supernatant, the procedure was repeated one more time with the addition of ice-cold PBS. After the second cycle, the pellet was resuspended in 500 µL of 1% CTAB buffer [24], followed by sonication at 35 kHz for 30 s (Bandelin, Germany) [25]. DNA extracts were normalised to 5 ng µL^{-1}, and the 16s rRNA gene V4 region was amplified using the primer set 515F and 806R [26] and then sequenced on the Illumina MiSeq platform by MrDNA (Molecular Research LP, Texas, USA). The samples from H-type cells with 15 g L^{-1} NaCl were discarded due to poor DNA yields. DADA2 within the QIIME2 platform was used to recover Amplicon Sequence Variants (ASVs), and the taxonomic assignment was performed based on the SILVA SSU Ref NR database release v. 138, according to a previously described protocol [27]. Taxa bars of the 25 most abundant microorganisms were plotted at the genus level using R's ggplot2 package. Beta diversity analyses were conducted by Principal Coordinates Analysis (PCoA) using the Bray-Curtis distance. The sequencing data is publicly available in the NCBI BioSample database (Bioproject ID PRJNA897847).

2.5. Chemical and electrochemical analyses

Conductivity was measured by an AET30 conductivity tester (Fisher Scientific, USA), whereas pH was monitored using a controller (Cole Parmer 300, UK) equipped with a slim pH probe (Hamilton, Switzerland). Liquid sample composition of catholyte and anolyte (carboxylic acids and alcohols) was determined by high-performance liquid chromatography (HPLC 1260 Infinity, Agilent Technology, USA) equipped with a Hi-Plex H column and refractive index detector (RID) as previously reported [28]. Na$^+$ concentrations were measured by Inductively Coupled Plasma−Optical Emission Spectroscopy (ICP-OES, Agilent 5110, US), whereas free chlorine concentrations were measured using DPD Free Chlorine Test N' Tube kits (Hach, USA). The gas produced was collected in gas bags, quantified by syringe and analysed (H$_2$, CO$_2$, and CH$_4$) by gas chromatography (GC 8860, Agilent Technologies, USA). The GC was equipped with serially connected GS-Carbon Plot and HP-PLOT Molesieve columns kept at 50 °C and with a thermal conductivity detector (TCD) kept at 150 °C. Helium was used as carrier gas at a flow rate of 2 mL min^{-1}.

The H-type cells were operated on a two-electrode configuration where the cell voltage was constantly monitored by the potentiostat. The anode potentials were measured on sampling days by using a multimeter after inserting a reference electrode (RS Pro RS12, Radionics, UK) in the anolyte. The three-chamber cells were operated on a three-electrode set-up where the cathode potential was constantly monitored, whereas the anode potential and cell voltage were measured on sampling days. The ohmic resistance of the cells was determined at the beginning of each run by two-electrode electric impedance spectroscopy (EIS) at 0 V, sinusoid amplitude of 10 mV, and frequency range for 0.1−100 kHz with ten measurement points per decade.

2.6. Calculations

Production rates between consecutive sampling days were calculated as the amount of acetate produced in the time unit (sum of acetate detected in catholyte and anolyte) normalised either to the catholyte volume or to the cathode projected surface. Specific productions were calculated as the ratio between acetate produced and electric power consumed. Coulombic efficiencies (CEs) were determined as the fraction of the total electrons supplied as the electric current, which were recovered as acetate. Carbon conversion efficiencies were calculated as the ratio between the carbon

introduced in the cell as CO$_2$ and the carbon recovered as acetate. All results, except those from the cell stack, are presented as the average and standard deviation of two independent cells operated under identical conditions. For the three-chamber cells, further statistic comparisons were performed by calculating the average production rate, CE, specific production, and carbon conversion efficiency during steady-state production periods at the different NaCl concentrations and current densities investigated. Significant differences were assessed by one-way analysis of variance (ANOVA) and the Tukey test ($p = 0.05$). The cathode potential of the H-type cells was estimated from the measured cell voltage and anode potential according to Ohm's law. Ohmic overpotentials were calculated as the product of ohmic resistance (measured by EIS) and applied current.

3. Results and discussion

3.1. Microbial electrosynthesis of acetate from bicarbonate at different salinity

The microbial community was successfully enriched for acetate production from bicarbonate at both 5 and 10 g L^{-1} initial NaCl concentration, defined as "moderate saline conditions" by the USGS [29]. In both cases, acetate was detected after 3−5 days lag-phase and accumulated to a total of 1.3 ± 0.3 and 1.4 ± 0.3 g L^{-1} in the duplicate cells with 5 and 10 g L^{-1} NaCl, respectively, by day 40 (Fig. 2). Higher NaCl concentrations of 15 and 20 g L^{-1} resulted in >90% lower acetate production (Fig. 2), suggesting the inhibition of the acetogenic microorganisms. Acetate was the only product detected in the cells, except for small amounts of formate (<0.2 g L^{-1}) found on the first days of operation and traces of propionate (<0.1 g L^{-1}) detected only in the cells with 5 g L^{-1} NaCl concentration.

Besides NaCl (5, 10, 15, or 20 g L^{-1}), other Na$^+$ sources, including NaHCO$_3$ and Na-BES, were introduced to the cell, resulting in an initial Na$^+$ concentration of 3.0 ± 0.0, 4.1 ± 0.2, 7.1 ± 0.0, and 8.8 ± 0.1 g L^{-1} Na$^+$, respectively. This resulted in initial catholyte conductivities of 17.5 ± 0.4, 22.3 ± 1.0, 34.9 ± 1.6, and 41.4 ± 3.2 mS cm^{-1}, respectively. Additional Na$^+$ was introduced to the catholyte as NaHCO$_3$ at the beginning of each fed-batch cycle and through the membrane by Na$^+$ migration from the anode [30], resulting in an increasing concentration trend. Na$^+$ migration was confirmed by its decreasing concentration in the anolyte (Fig. 2) and by the increasing and decreasing conductivity trend in the catholyte and anolyte, respectively (Fig. S2 in the Supplementary material). The results obtained herein (Fig. 2) suggested that concentrations above 6 g L^{-1} Na$^+$ inhibited the acetogenic members of the microbial community in this study, resulting in poor acetate production in the cells started up with more than 10 g L^{-1} NaCl. Previous studies on anaerobic digestion showed that certain mixed cultures of acetogens could metabolize at Na$^+$ concentrations of 24 g L^{-1} [31], although the inhibitory threshold depends on the microorganisms. Furthermore, MES cells are prone to additional stress conditions, such as O$_2$ intrusion from the anode compartment, which may contribute to microbial inhibition and cause product oxidation [32]. When using a saline electrolyte, another issue could be the production of chlorinated species (i.e., Cl$_2$, HClO) at the anode, which can then diffuse towards the cathode. However, cathodic concentrations of only 4.2 (± 2.9) mg L^{-1} free chlorine were detected in the worst-case scenario (cells started up with 20 g L^{-1} NaCl), which appears too low to cause inhibition [33].

Higher salinity in the electrolyte, and thus the higher conductivity of the medium, resulted in a lower ohmic resistance of the cell (normalised per electrochemically active surface area), which was estimated as 260.6 ± 5.8, 169.2 ± 9.4, 120.2 ± 14.4, and
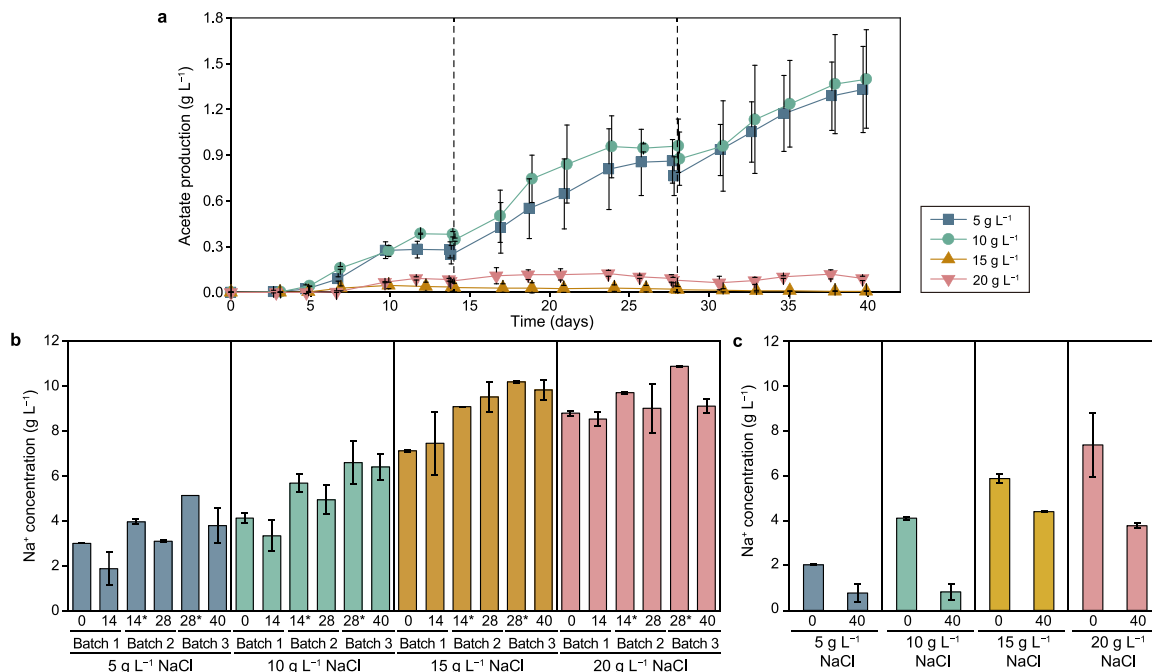
Fig. 2. a, Acetate production profiles of the H-type MES cells at different initial NaCl concentrations. **b–c**, Na$^+$ concentration in the catholyte (**b**) and in the anolyte (**c**) at the beginning and the end of each fed-batch cycle (days 0–14, 14–28, and 28–40). The asterisks represent the Na$^+$ concentration after feeding 4 g L^{-1} NaHCO$_3$ at the beginning of each fed-batch cycle.

93.4 ± 11.3 mΩ m^2 with a NaCl concentration of 5, 10, 15 and 20 g L^{-1}, respectively, based on EIS analysis (Fig. S3 in the Supplementary material). This resulted in an ohmic overpotential decreasing from 0.33 ± 0.01 V (with 5 g L^{-1} NaCl) to 0.21 ± 0.02 V (with 10 g L^{-1} NaCl) and further to 0.12 ± 0.01 V (with 20 g L^{-1} NaCl). Thus, the cells with 10 g L^{-1} NaCl were electrically more efficient than those with 5 g L^{-1} NaCl, requiring a lower voltage (2.5–2.6 V) to deliver the same current of 0.25 mA cm^{-2} to the cathode (Table 1). This resulted in a maximum acetate-specific production of 58.4 kg MWh^{-1}, 24% higher than that obtained with 5 g L^{-1} NaCl (46.8 kg MWh^{-1}). Despite the higher applied current (0.25 vs 0.156 mA cm^{-2}), the cell voltage was similar to that reported by Zhang et al. [21] in two-chamber cells at 35 g L^{-1} salinity, suggesting that the addition of more than 10 g L^{-1} NaCl might not improve the efficiency of the cells significantly.

Similar CE was obtained for acetate production at the two NaCl concentrations, which averaged 43% and 46% in the cells with 5 and 10 g L^{-1} NaCl, respectively, in the second at third fed-batch cycles. This confirms the capability of the microbial community to reduce CO$_2$ to acetate with similar efficiency under both salinity conditions and that higher salinity may help decrease the power demand of the cells as long as inhibitory conditions are not reached. Furthermore, the microbial communities showed resilience towards the cathode potential, which fluctuated between −1.15 and −1.46 V and between −1.04 and −1.48 V vs Ag/AgCl in the cells with initial NaCl concentrations of 5 and 10 g L^{-1} NaCl, and pH, which increased over time and occasionally exceeded pH 9 before being adjusted back to 6 (Fig. S4 in the Supplementary material).

3.2. CO$_2$ conversion to acetate in three-chamber microbial electrosynthesis cells

The planktonic communities enriched for acetogenesis at 5 and 10 g L^{-1} initial NaCl concentrations with the H-type cells were used as inoculum (10% v/v) for three-chamber CO$_2$-fed cells, where both catholyte and anolyte compositions were the same used in the previous experiment. The cells were initially operated at the same specific applied current of 0.25 mA cm^{-2} (16 mA). Acetate was

Table 1
Key performance parameters of the cells operated in galvanostatic mode (0.25 mA cm^{-2}) with an initial concentration of 5 and 10 g L^{-1} NaCl in both catholyte and anolyte. The results shown refer to the average of duplicate cells for linear (R^2 > 0.96) acetate production over time.

NaCl concentration (g L^{-1})	Fed-batch cycle	Operation days[a]	Conductivity (mS cm^{-1})	Acetate production rate		Average cell voltage (V)	Specific production (kg MWh^{-1})	Coulombic efficiency (%)
				g m^{-2} d^{-1}	mg L^{-1} d^{-1}			
5	1	5–10	17.0	6.5	52.0	2.63	40.3	38
	2	14–21	21.7	7.2	57.4	2.65	44.3	42
	3	28–35	26.4	7.4	59.3	2.65	46.8	44
10	1	5–10	22.7	5.7	45.4	2.58[b]	36.2	34
	2	14–21	28.2	9.3	74.3	2.52	58.4	52
	3	28–35	32.3	6.8	54.5	2.57	42.3	39

[a] Steady-state acetate production periods.
[b] This value refers to only one cell due to a measurement problem in the replicate cell. Full voltage profiles are available in Fig. S4 in the Supplementary material.

detected from day 5 onwards in the cells with an initial NaCl concentration of 5 g L^{-1} NaCl, whereas no significant acetate production was detected until day 10 in the cells started-up with 10 g L^{-1} NaCl (Fig. 3). This disagrees with the results obtained in the H-type cells, where no difference was detected in the start-up times of the cells with 5 or 10 g L^{-1} NaCl. It is plausible that the larger membrane area of the GDE cells resulted in a higher oxygen cross-over towards the cathode than in the H-type cells. This introduced further stress to the organisms, resulting in a slower start-up. Furthermore, several attempts to inoculate the three-chamber cells directly with the anaerobic sludge failed, suggesting that a pre-enrichment in the H-type cells was required for a successful start-up [34].

After start-up, acetate was linearly produced (Fig. 3) at an average rate of 7.7 and 5.5 g m^{-2} d^{-1} (0.12 and 0.09 g L^{-1} d^{-1}) in the cells with initial NaCl concentrations of 5 and 10 g L^{-1}, with average CEs of 46.1% and 32.5%, respectively (Fig. 4). Continuous CO$_2$ sparging resulted in a relatively stable pH (Fig. 3), which did not increase over time as occurred in the bicarbonate-fed H-type cells. The catholyte pH even slowly decreased to around 6 in the cells with 5 g L^{-1} NaCl as a consequence of acetate accumulation, whereas it remained higher (6.4) in the cells with 10 g L^{-1} NaCl due to the slower acetate production (Fig. 3). The anode pH stabilized to around 2 with 5 g L^{-1} NaCl, and was even lower in the cells with 10 g L^{-1} NaCl (Fig. S5 in the Supplementary material). Neither hydrogen nor methane was detected in the cathode outlet gas, mainly consisting of residual CO$_2$, with a small concentration of oxygen (<1%) likely diffusing from the anodic chamber through the Nafion membrane. In MES cells inoculated with mixed cultures, facultative microorganisms consume the oxygen diffusing through the membrane, avoiding inhibition of the anaerobic members of the community, although at the expense of the CE [11].

Since the absence of hydrogen in the cathode headspace suggested that the biocatalyst can support higher current densities, the applied current was increased four times to 1 mA cm^{-2} (64 mA). In the cells with an initial NaCl concentration of 5 g L^{-1}, increasing four-fold the current input resulted in an over seven-fold higher average acetate production rate of 48.3 g m^{-2} d^{-1} (0.77 g L^{-1} d^{-1}) with a peak of 55.4 g m^{-2} d^{-1} (0.89 g L^{-1} d^{-1}) (Fig. 4). In fact, besides providing more reducing equivalents, increasing the current improved the CE to an average of 71.9% on days 17−24, with a maximum of 82.4%. The average carbon conversion efficiency achieved under those conditions was 8%, suggesting that gas recirculation [35] and/or connecting several cells in series will be required to achieve full conversion. From day 24 onwards, the

production rate decreased due to acetate accumulation (>5 g L^{-1}) in the catholyte (Fig. S5 in the Supplementary material). The gradual inhibition of the acetogenic community was confirmed by the increasing share of electrons escaping the cell as hydrogen gas (Fig. 4), which was detected only at low concentrations when acetogenesis was occurring at the highest rate. Nonetheless, acetate production occurred until day 33, despite the pH as low as 4.3 and acetate concentrations of 5.5 (± 0.8) g L^{-1} in the catholyte.

The acetate production rate per electrode surface achieved in this study was comparable to that obtained in a previous study with GDE in a three-chamber cell [23]. With a similar set-up, Srikanth et al. [13] obtained a peak carboxylic acid production rate of 23 g m^{-2} d^{-1} (including formate, acetate and butyrate), as well as alcohol (methanol, ethanol and butanol) production rates up to 11.7 g m^{-2} d^{-1}. Conversely, in this study, acetate was the only product (>99% on a carbon basis), which can be attributed to the different origins of microorganisms (anaerobic sludge adapted to salinity vs corroded metal piece). A higher production rate can potentially be achieved by modifying the GDE surface, e.g., by doping with conductive polymers [36] or carbon nanotubes [37] to sustain higher current densities. The average CE obtained in this study was higher than in similar studies with GDE [13,23], confirming that adding 5 g L^{-1} NaCl had no negative impact on the acetogenic community. Higher CEs approaching 100% can be achieved by promoting the formation of a dense cathodic biofilm [8,38].

In the cells with initial NaCl concentration of 10 g L^{-1}, four-time higher applied current resulted in only 4.2-time higher acetate production rate to an average of 23.4 g m^{-2} d^{-1} (0.37 g L^{-1} d^{-1}), without any significant CE increase (Fig. 4). Furthermore, the production rate declined four days after increasing the current density, despite the catholyte pH of 6.2−6.5 (Fig. 3) was within an optimal range for acetogenesis in electrosynthetic microbiomes [39], resulting in the increasing amounts of unused hydrogen (Fig. 4). This was likely due to the high Na$^+$ concentration in the catholyte, which was above 5 g L^{-1} at the beginning of the experiment and increased to around 6 g L^{-1} after the current increase (Fig. 3), causing inhibition as occurred in the experiment with the H-type cells (Fig. 2). This increase of concentration was due to the migration of Na$^+$ ions from the anolyte towards the catholyte, as suggested by the sharp decrease of Na$^+$ concentration in the anolyte after the current increase (Fig. 3). Free chlorine concentration in the catholyte remained low (2.3 ± 1.3 mg L^{-1}) and unlikely to cause inhibition.

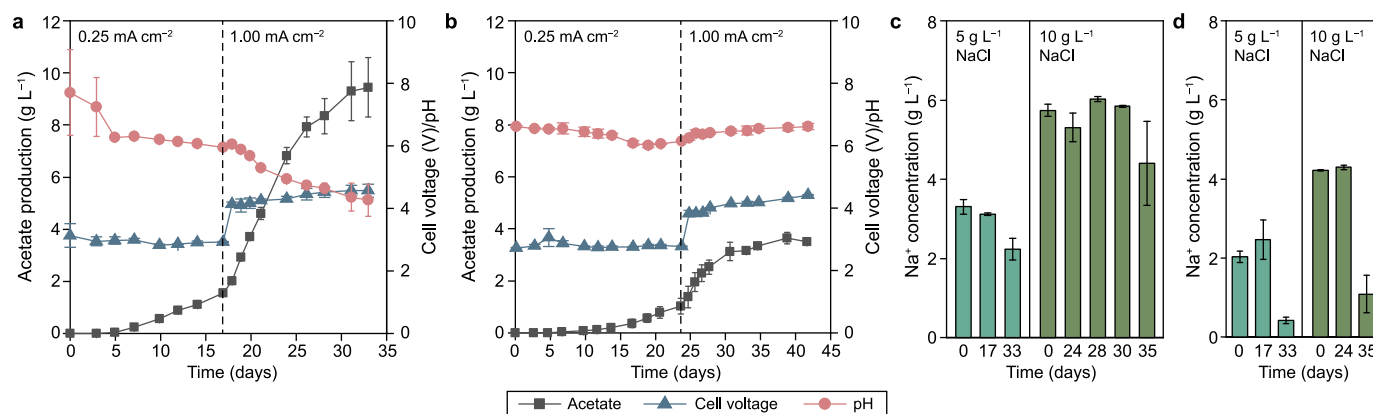The three-chamber cell configuration was characterised by a

Fig. 3. a−b, Acetate production (primary y-axis), cell voltage and pH profile (secondary y-axis) of the three-chamber MES cells operated with initial NaCl concentrations of 5 g L^{-1} (**a**) and 10 g L^{-1} (**b**). **c−d**, Na$^+$ concentration in the catholyte (**c**) and anolyte (**d**) on different operation days.
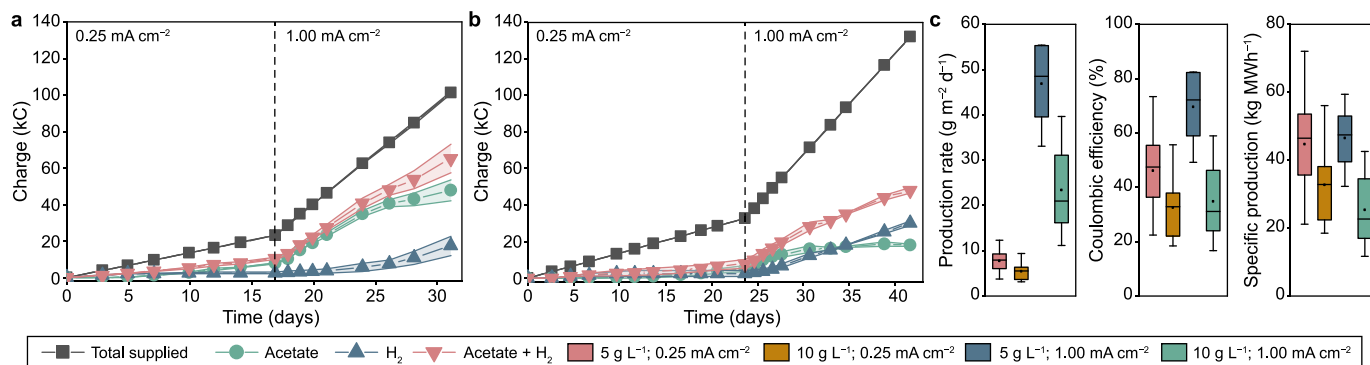
Fig. 4. a–b, Charge distribution over time in the three-chamber MES cells operated with initial NaCl concentrations of 5 g L^{-1} (**a**) and 10 g L^{-1} (**b**). **c,** Box plots representing the steady-state average (dots), median (line), first and third quartile (box), and minimum/maximum values (whiskers) of several performance parameters under different operation conditions.

more efficient design than the H-type cell, with a much higher cathode area/volume ratio (0.032 against 0.008 m^2 L^{-1}) and a lower distance between the anode and cathode electrode (around 5 cm). This resulted in lower ohmic resistances with respect to the H-type cells (139.5 ± 0.0 and 82.6 ± 8.3 mΩ m^2 at NaCl concentrations of 5 and 10 g L^{-1}, respectively) (Fig. S3 in the Supplementary material). Ohmic resistances of only 2.4 mΩ m^2 have been reported for a vapour-fed, zero-gap methanogenic MES [40]. Such efficient design allows substantial energy saving, but further experiments with larger electrodes and longer operation times are required to confirm its potential for scale-up.

At an applied current density of 0.25 mA cm^{-2}, the cells with 5 and 10 g L^{-1} NaCl stabilized to a relatively constant cell voltage of 2.94 ± 0.06 and 2.80 ± 0.09 V, respectively (Fig. 3), with cathode potentials around −0.9 V vs Ag/AgCl in both cases (Fig. S6 in the Supplementary material). Despite the 5% higher power consumption, the cells with 5 g L^{-1} NaCl initial concentration reached a higher average specific production (44.7 kg MWh^{-1}) than the cells with 10 g L^{-1} NaCl (32.7 kg MWh^{-1}) due to the higher CE (Fig. 4). The difference was even more evident after increasing the current to 1 mA cm^{-2}, where the productivity of the cells with 5 g L^{-1} NaCl (48.0 kg MWh^{-1}) was significantly higher than that obtained at 10 g L^{-1} NaCl (25.3 kg MWh^{-1}), despite the higher average cell voltage (4.34 ± 0.19 V against 4.08 ± 0.22 V).

3.3. MES cell stack

As a proof of concept, a working MES with active acetogenic microorganisms was hydraulically connected in series to two additional cells to simulate a stack of three cells, although maintaining independent gas and power lines. Cell stacks are the most efficient way to scale up electrochemical systems, as the efficiency unavoidably increases with the cell size [41]. An average acetate production rate of 7.8 ± 0.6 g m^{-2} d^{-1} was obtained at 0.25 mA cm^{-2} on days 3−10, with a CE of 46.6 ± 3.6% (Fig. 5). Such production rate is similar to that obtained in the single cell (Fig. 4) but, being normalised to the surface of three electrodes, indicated a three-times higher acetate production. The specific acetate production obtained was 46.3 kg MWh^{-1}. This result confirms that an MES stack can be easily and quickly started up by enriching the autotrophic community in a single cell and then circulating the catholyte to the other modules without the need for inoculating each cell separately. After increasing the current input of the three cells to 1 mA cm^{-2}, the production rate increased to a maximum of 33.0 g m^{-2} d^{-1} (Fig. 5). Such production rate is 40% lower than the highest production rate obtained with the single cells (Fig. 4),

suggesting that the community was unable of consuming the hydrogen produced by the three electrodes at 1 mA cm^{-2} applied current. Furthermore, the acetate production rate declined on day 13, likely due to the quick acidification of the catholyte, which can be counteracted by in-line product extraction [42].

3.4. Microbial community analysis

SEM images revealed the presence of scattered cells on the carbon cloth cathode of the H-type cells, whereas a more compact though non-homogeneous biofilm was observed on the GDE surface (Fig. S7 in the Supplementary material). Since the H$_2$ solubility decreases with salt concentration, developing a biofilm capable of capturing the H$_2$ produced at the cathode is imperative in systems operated under saline conditions. In both H-type and GDE cells, the microorganisms identified were mainly rod-shaped. *Acetobacterium* sp. was the key acetogenic microorganism in the H-type cells with either 5 or 10 g L^{-1} NaCl initial concentration, with an average relative abundance of about 25% in both cases (Fig. 6), which justifies the similar acetate production rates achieved under the two conditions (Fig. 2). Beta diversity analysis (Fig. S8 in the Supplementary material) confirmed that similar communities were enriched with 5 and 10 g L^{-1} NaCl initial concentration, whereas the communities selected with 20 g L^{-1} NaCl clustered separately. In particular, the *Acetobacterium* quota declined to 9 ± 3% with 20 g L^{-1} initial NaCl concentration, causing poor acetate production, despite the increased relative abundance of *Acetoanaerobium* sp., an acetogenic bacterium previously isolated from saline environments [43], whose abundance exceed 15% in one of the replicate cells.

The relative abundance of *Acetobacterium* sp. was substantially higher in the three-chamber cells, where it dominated the community (76.3 ± 19.4% and 70.8 ± 10.0% with 5 and 10 g L^{-1} NaCl initial concentration, respectively), resulting in the relatively high CEs achieved (Fig. 4). *Acetobacterium* has been widely indicated as one of the key species in the core microbiome of acetogenic MES cells, and responsible of acetate production from CO$_2$ and (bio) electrochemically produced H$_2$ through the Wood-Ljungdahl Pathway [44]. It has been reported to dominate the cathodic community of MES cells operated at up to 60 g L^{-1} salinity [21], demonstrating resilience to halophilic conditions. The hydrogen-producing *Desulfovibrio* sp., a syntrophic partner of *Acetobacterium*, was detected in both the H-type and the three-chamber cells at relative abundances between 1% and 3%, along with the other members of the MES core microbiomes (*Christensenellaceae*, *Lentimicrobiaceae*, and *Synergistaceae*) [4]. This suggests that
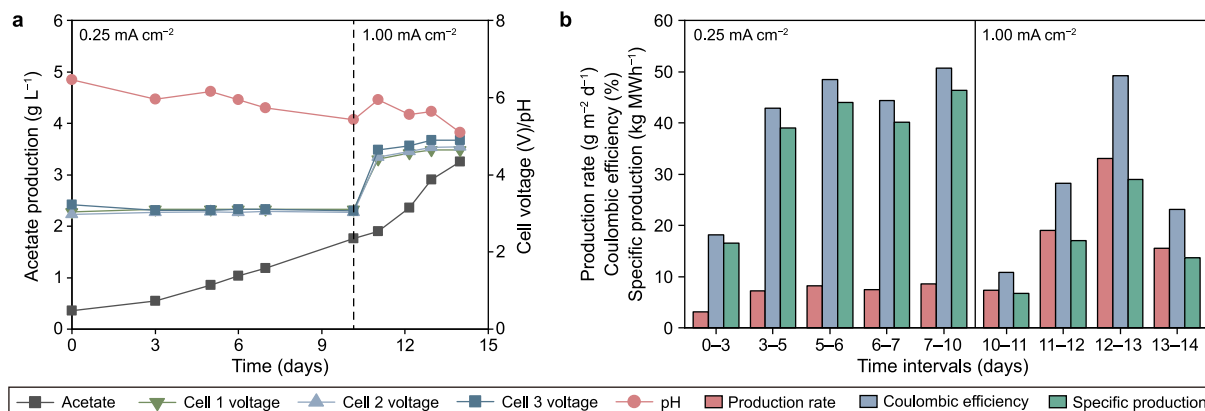
Fig. 5. a, Acetate production (primary y-axis), cells voltage and pH profile (secondary y-axis) of the three-chamber MES cell stack operated with initial NaCl concentrations of 5 g L^{-1} **b**, Production rates, Coulombic efficiencies, and specific production of the cell stack over time.
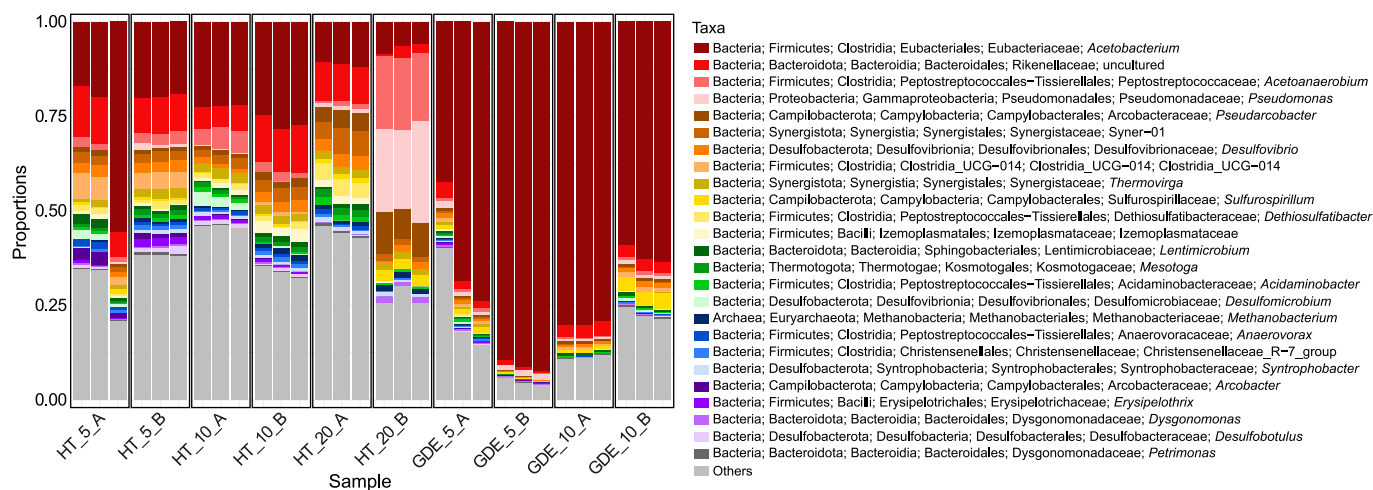

Fig. 6. Taxa bars depicting the cathodic community composition in the H-type (HT) and three-chamber (GDE) cells started at different NaCl concentrations (5, 10, or 20 g L^{-1}). A and B refer to the two replicate cells of each experiment. H-type cells with 15 g L^{-1} NaCl were excluded from the analysis due to insufficient DNA yields. The family and genus of each microorganism are shown in the legend. "Others" represents the sum of the relative abundance of microorganisms outside the top-25.

concentrations up to 10 g L^{-1} NaCl can be added to increase the catholyte conductivity without a major impact on the core microbiome of acetogenic MES. Among the other microorganisms, several aerobic/microaerophilic species, including *Sulfurospirillum* and *Pseudomonas*, were detected in both H-type and three chamber cells, likely involved in oxygen scavenging roles.

3.5. Practical implications

This study indicated that three-chamber MES cells equipped with GDEs are an efficient and scalable technology to bring MES towards commercialisation and that moderate saline conditions (5 g L^{-1} NaCl) can help decrease the electric power input required for CO$_2$ reduction. Galvanostatic operation allows control of the production rates and does not require a reference electrode, representing a better solution than potentiostatic operation when strict potential control is not required. In this study, H$_2$-mediated CO$_2$ reduction to acetate was indeed efficient in a wide range of cathode potentials (from −0.9 V to −1.4 V vs Ag/AgCl at 0.25 and 1.00 mA cm^{-2}, respectively). Finally, the first proof of concept of a GDE-based MES stack was provided, showing that the microbial consortia enriched in a single cell can be circulated to inoculate the

entire stack, facilitating efficient start-up. Despite the promising results, several challenges remain to take MES technology towards commercialisation.

- A current density of 1 mA cm^{-2} was used in this study, whereas 1−2 orders of magnitude higher current densities are required to avoid excessive capital costs. Higher current densities are achievable by increasing the electrode surface and promoting the development of a thick biofilm [38]. However, this must be accompanied by the development of efficient product extraction and H$^+$ selective membranes to avoid the accumulation of products and cross-over of oxygen and competing cations.

- Based on the current acetate market value of €0.4−0.7 ton^{-1} [45] and non-household electric energy cost of around €144 MWh^{-1}, including taxes [46], the obtained acetate production of 50−60 kg MWh^{-1} is at least four times lower than that required for economic feasibility. The competitiveness of MES will benefit from the development and rapidly decreasing cost of renewable energy, but this could not be enough. Research efforts must be directed to produce more valuable products than acetate (e.g., caproic acid or hexanol) at a high rate and develop more efficient cell and electrode designs to reduce

overpotentials and increase the CE. In this regard, 3D printing is a valuable research tool to test optimised MES cell configurations.

- This study was conducted with pure CO_2 and low flow rates, with only 8% carbon conversion efficiency achieved and a few grams of carbon treated per day. Higher efficiencies can be achieved using 3D structured cathodes, operating the cells with gas recirculation and connecting multiple cells in series. Further studies with real industrial flue gases delivered to the MES cells at high flow rates should be conducted. Although promising in terms of circular bioeconomy, MES technology appears immature to reach plant capacities to treat tons of CO_2 per day, as required by carbon-intensive industries.

4. Conclusions

This study shows that NaCl-based electrolytes can help decrease the electric power demand of MES cells without compromising their conversion efficiency, but Na^+ concentrations higher than 6 g L^{-1} must be avoided when relying on non-halophilic microorganisms. Three-chamber cells equipped with GDEs evolved an efficient cathodic community dominated by *Acetobacterium* that achieved CO_2 conversion to acetate with the highest production rate of 55.4 g m^{-2} d^{-1}, exceeding 80% Coulombic efficiency at 1 mA cm^{-2} applied current. The enriched microbial community in the catholyte can act as an inoculum to achieve acetate production in further cells with a minimum lag phase. Such modular cells can be stacked by serial hydraulic connection obtaining a proportional increase in acetate production. However, developing H^+ selective membranes and efficient in-line product extraction is required, particularly at high current density, to avoid a quick deterioration of the production rate due to product inhibition, ion migration, and oxygen cross-over.

CRediT author contribution statement

Paolo Dessì: Conceptualization, Investigation, Writing - original draft, Project administration, Funding acquisition. **Claribel Buenaño-Vargas:** Methodology, Visualization, Writing - review & editing. **Santiago Martínez-Sosa:** Investigation, Writing - review & editing. **Simon Mills:** Methodology, Writing - review & editing. **Anna Trego:** Methodology, Writing - review & editing. **Umer Z. Ijaz:** Methodology, Writing - review & editing. **Deepak Pant:** Resources, Writing - review & editing. **Sebastià Puig:** Writing - review & editing. **Vincent O'Flaherty:** Writing - review & editing. **Pau Farràs:** Conceptualization, Project administration, Funding acquisition, Writing - review & editing.

Declaration of competing interest

The authors declare that they have no known competing financial interests or personal relationships that could have appeared to influence the work reported in this paper.

Appendix A. Supplementary data

Supplementary data to this article can be found online at https://doi.org/10.1016/j.ese.2023.100261.

References

[1] K.P. Nevin, T.L. Woodard, A.E. Franks, Z.M. Summers, D.R. Lovley, Microbial electrosynthesis: feeding microbes electricity to convert carbon dioxide and water to multicarbon extracellular organic compounds, mBio 1 (2010) e00103–e00110, https://doi.org/10.1128/mBio.00103-10.

[2] B.E. Logan, R. Rossi, A. Ragab, P.E. Saikaly, Electroactive microorganisms in bioelectrochemical systems, Nat. Rev. Microbiol. 17 (2019) 307–319, https://doi.org/10.1038/s41579-019-0173-x.

[3] C.W. Marshall, D.E. Ross, K.M. Handley, P.B. Weisenhorn, J.N. Edirisinghe, C.S. Henry, J.A. Gilbert, H.D. May, R.S. Norman, Metabolic reconstruction and modeling microbial electrosynthesis, Sci. Rep. 7 (2017) 8391, https://doi.org/10.1038/s41598-017-08877-z.

[4] S. Mills, P. Dessì, D. Pant, P. Farràs, W.T. Sloan, G. Collins, U.Z. Ijaz, A meta-analysis of acetogenic and methanogenic microbiomes in microbial electrosynthesis, NPJ Biofilms Microbiomes 8 (2022) 73, https://doi.org/10.1038/s41522-022-00337-5.

[5] L. Rovira-Alsina, M. Dolors Balaguer, S. Puig, Transition roadmap for thermophilic carbon dioxide microbial electrosynthesis: testing with real exhaust gases and operational control for a scalable design, Bioresour. Technol. 365 (2022), 128161, https://doi.org/10.1016/j.biortech.2022.128161.

[6] A. Prévoteau, J.M. Carvajal-Arroyo, R. Ganigué, K. Rabaey, Microbial electrosynthesis from CO_2: forever a promise? Curr. Opin. Biotechnol. 62 (2020) 48–57, https://doi.org/10.1016/j.copbio.2019.08.014.

[7] B.D. Virdis, R. Hoelzle, A. Marchetti, S.T. Boto, M.A. Rosenbaum, R. Blasco-Gómez, S. Puig, S. Freguia, M. Villano, Electro-fermentation: sustainable bio-productions steered by electricity, Biotechnol. Adv. 59 (2022), 107950, https://doi.org/10.1016/j.biotechadv.2022.107950.

[8] F. Kracke, J.S. Deutzmann, B.S. Jayathilake, S.H. Pang, S. Chandrasekaran, S.E. Baker, A.M. Spormann, Efficient hydrogen delivery for microbial electrosynthesis via 3D-printed cathodes, Front. Microbiol. 12 (2021), 696473, https://doi.org/10.3389/fmicb.2021.696473.

[9] A. Krige, U. Rova, P. Christakopoulos, 3D bioprinting on cathodes in microbial electrosynthesis for increased acetate production rate using *Sporomusa ovata*, J. Environ. Chem. Eng. 9 (2021), 106189, https://doi.org/10.1016/j.jece.2021.106189.

[10] N.J. Claassens, C.A.R. Cotton, D. Kopljar, A. Bar-Even, Making quantitative sense of electromicrobial production, Nat Catal 2 (2019) 437–447, https://doi.org/10.1038/s41929-019-0272-0.

[11] I. Vassilev, P. Dessì, S. Puig, M. Kokko, Cathodic biofilms − a prerequisite for microbial electrosynthesis, Bioresour. Technol. 348 (2022), 126788, https://doi.org/10.1016/j.biortech.2022.126788.

[12] D. Higgins, C. Hahn, C. Xiang, T.F. Jaramillo, A.Z. Weber, Gas-diffusion electrodes for carbon dioxide reduction: a new paradigm, ACS Energy Lett. 4 (2019) 317–324, https://doi.org/10.1021/acsenergylett.8b02035.

[13] S. Srikanth, D. Singh, K. Vanbroekhoven, D. Pant, M. Kumar, S.K. Puri, S.S.V. Ramakumar, Electro-biocatalytic conversion of carbon dioxide to alcohols using gas diffusion electrode, Bioresour. Technol. 265 (2018) 45–51, https://doi.org/10.1016/j.biortech.2018.02.058.

[14] W. Wei, J. Xu, W. Chen, L. Mi, J. Zhang, A review of sodium chloride-based electrolytes and materials for electrochemical energy technology, J Mater Chem A Mater 10 (2022) 2637–2671, https://doi.org/10.1039/d1ta09371a.

[15] N. Gunde-Cimerman, A. Plemenitaš, A. Oren, Strategies of adaptation of microorganisms of the three domains of life to high salt concentrations, FEMS Microbiol. Rev. 42 (2018) 353–375, https://doi.org/10.1093/femsre/fuy009.

[16] H.L. Drake, K. Küsel, C. Matthies, Acetogenic Prokaryotes, the Prokaryotes: Prokaryotic Physiology and Biochemistry, 2013, https://doi.org/10.1007/978-3-642-30141-4_61.

[17] K. Schuchmann, V. Müller, Autotrophy at the thermodynamic limit of life: a model for energy conservation in acetogenic bacteria, Nat. Rev. Microbiol. 12 (2014) 809–821, https://doi.org/10.1038/nrmicro3365.

[18] J. Philips, K. Rabaey, D.R. Lovley, M. Vargas, Biofilm formation by *Clostridium ljungdahlii* is induced by sodium chloride stress: Experimental evaluation and transcriptome analysis, PLoS One 12 (2017) 1–25, https://doi.org/10.1371/journal.pone.0170406.

[19] M.F. Alqahtani, S. Bajracharya, K.P. Katuri, M. Ali, J. Xu, M.S. Alarawi,

P.E. Saikaly, Enrichment of salt-tolerant CO$_2$−fixing communities in microbial electrosynthesis systems using porous ceramic hollow tube wrapped with carbon cloth as cathode and for CO$_2$ supply, Sci. Total Environ. 766 (2021), 142668, https://doi.org/10.1016/j.scitotenv.2020.142668.

[20] M.F. Alqahtani, S. Bajracharya, K.P. Katuri, M. Ali, A. Ragab, G. Michoud, D. Daffonchio, P.E. Saikaly, Enrichment of *Marinobacter* sp. and halophilic homoacetogens at the biocathode of microbial electrosynthesis system inoculated with red sea brine pool, Front. Microbiol. 10 (2019) 1−18, https://doi.org/10.3389/fmicb.2019.02563.

[21] X. Zhang, T. Arbour, D. Zhang, S. Wei, K. Rabaey, Microbial electrosynthesis of acetate from CO$_2$ under hypersaline conditions, Environmental Science and Ecotechnology 100211 (2023), https://doi.org/10.1016/j.ese.2022.100211.

[22] M. Isipato, P. Dessì, C. Sánchez, S. Mills, U.Z. Ijaz, F. Asunis, D. Spiga, G. de Gioannis, M. Mascia, G. Collins, A. Muntoni, P.N.L. Lens, Propionate production by bioelectrochemically-assisted lactate fermentation and simultaneous CO$_2$ recycling, Front. Microbiol. 11 (2020) 1−16, https://doi.org/10.3389/fmicb.2020.599438.

[23] S. Bajracharya, K. Vanbroekhoven, C.J.N. Buisman, D. Pant, D.P.B.T.B. Strik, Application of gas diffusion biocathode in microbial electrosynthesis from carbon dioxide, Environ. Sci. Pollut. Control Ser. 23 (2016) 22292−22308, https://doi.org/10.1007/s11356-016-7196-x.

[24] R.I. Griffiths, A.S. Whiteley, A.G. O'Donnell, M.J. Bailey, Rapid method for coextraction of DNA and RNA from natural environments for analysis of ribosomal DNA- and rRNA-based microbial community composition, Appl. Environ. Microbiol. 66 (2000) 5488−5491, https://doi.org/10.1128/AEM.66.12.5488-5491.2000.

[25] C. Keating, J.P. Chin, D. Hughes, P. Manesiotis, D. Cysneiros, T. Mahony, C.J. Smith, J.W. McGrath, V. O'Flaherty, Biological phosphorus removal during high-rate, low-temperature, anaerobic digestion of wastewater, Front. Microbiol. 7 (2016) 1−14, https://doi.org/10.3389/fmicb.2016.00226.

[26] J.G. Caporaso, C.L. Lauber, W.A. Walters, D. Berg-Lyons, C.A. Lozupone, P.J. Turnbaugh, N. Fierer, R. Knight, Global patterns of 16S rRNA diversity at a depth of millions of sequences per sample, Proc. Natl. Acad. Sci. U. S. A. 108 (2011) 4516−4522, https://doi.org/10.1073/pnas.1000080107.

[27] A.C. Trego, B.C. Holohan, C. Keating, A. Graham, S. O'Connor, M. Gerardo, D. Hughes, U.Z. Ijaz, V. O'Flaherty, First proof of concept for full-scale, direct, low-temperature anaerobic treatment of municipal wastewater, Bioresour. Technol. 341 (2021), 125786, https://doi.org/10.1016/j.biortech.2021.125786.

[28] P. Dessì, C. Sánchez, S. Mills, F.G. Cocco, M. Isipato, U.Z. Ijaz, G. Collins, P.N.L. Lens, Carboxylic acids production and electrosynthetic microbial community evolution under different CO$_2$ feeding regimens, Bioelectrochemistry 137 (2021b), 107686, https://doi.org/10.1016/j.bioelechem.2020.107686.

[29] D.G. Driscoll, J.M. Carter, J.E. Williamson, L.D. Putnam, Hydrology of the Black Hills Area, South Dakota, 2002.

[30] M. Zeppilli, P. Paiano, C. Torres, D. Pant, A critical evaluation of the pH split and associated effects in bioelectrochemical processes, Chem. Eng. J. 422 (2021), 130155, https://doi.org/10.1016/j.cej.2021.130155.

[31] Y. Zhang, L. Li, X. Kong, F. Zhen, Z. Wang, Y. Sun, P. Dong, P. Lv, Inhibition effect of sodium concentrations on the anaerobic digestion performance of *Sargassum* species, Energy Fuel. 31 (2017) 7101−7109, https://doi.org/10.1021/acs.energyfuels.7b00557.

[32] M. Abdollahi, S. al Sbei, M.A. Rosenbaum, F. Harnisch, The oxygen dilemma: the challenge of the anode reaction for microbial electrosynthesis from CO$_2$,

Front. Microbiol. 13 (2022), 947550, https://doi.org/10.3389/fmicb.2022.947550.

[33] Z. Shao, X. Guo, Q. Qu, K. Kang, Q. Su, C. Wang, L. Qiu, Effects of chlorine disinfectants on the microbial community structure and the performance of anaerobic digestion of swine manure, Bioresour. Technol. 339 (2021), 125576, https://doi.org/10.1016/j.biortech.2021.125576.

[34] M. Rojas, P.A. del, M. Zaiat, E.R. González, H. de Wever, D. Pant, Enhancing the gas−liquid mass transfer during microbial electrosynthesis by the variation of CO$_2$ flow rate, Process Biochem. 101 (2021) 50−58, https://doi.org/10.1016/j.procbio.2020.11.005.

[35] R. Mateos, A. Sotres, R.M. Alonso, A. Morán, A. Escapa, Enhanced CO$_2$ conversion to acetate through microbial electrosynthesis (MES) by continuous headspace gas recirculation, Energies 12 (2019) 3297.

[36] J.M. Fontmorin, P. Izadi, D. Li, S.S. Lim, S. Farooq, S.S. Bilal, S. Cheng, E.H. Yu, Gas diffusion electrodes modified with binary doped polyaniline for enhanced CO$_2$ conversion during microbial electrosynthesis, Electrochim. Acta 372 (2021), 137853, https://doi.org/10.1016/J.ELECTACTA.2021.137853.

[37] V. Flexer, L. Jourdin, Purposely designed hierarchical porous electrodes for high rate microbial electrosynthesis of acetate from carbon dioxide, Acc. Chem. Res. 53 (2020) 311−321, https://doi.org/10.1021/acs.accounts.9b00523.

[38] L. Jourdin, S.M.T. Raes, C.J.N. Buisman, D.P.B.T.B. Strik, Critical biofilm growth throughout unmodified carbon felts allows continuous bioelectrochemical chain elongation from CO$_2$ up to caproate at high current density, Front. Energy Res. 6 (2018) 7, https://doi.org/10.3389/fenrg.2018.00007.

[39] E. v Labelle, C.W. Marshall, J.A. Gilbert, H.D. May, Influence of acidic pH on hydrogen and acetate production by an electrosynthetic microbiome, PLoS One 9 (2014), e109935, https://doi.org/10.1371/journal.pone.0109935.

[40] G. Baek, R. Rossi, P.E. Saikaly, B.E. Logan, High-rate microbial electrosynthesis using a zero-gap flow cell and vapor-fed anode design, Water Res. 219 (2022), 118597, https://doi.org/10.1016/j.watres.2022.118597.

[41] J. Greenman, I.A. Ieropoulos, Allometric scaling of microbial fuel cells and stacks: the lifeform case for scale-up, J. Power Sources 356 (2017) 365−370, https://doi.org/10.1016/j.jpowsour.2017.04.033.

[42] P. Dessì, L. Rovira-Alsina, C. Sánchez, G.K. Dinesh, W. Tong, P. Chatterjee, M. Tedesco, P. Farràs, H.V.M. Hamelers, S. Puig, Microbial electrosynthesis: towards sustainable biorefineries for production of green chemicals from CO$_2$ emissions, Biotechnol. Adv. 46 (2021a), 107675, https://doi.org/10.1016/j.biotechadv.2020.107675.

[43] C. Martin, Genomic Analysis of *Acetoanaerobium* Sp. VLB-1, an Anaerobic Bacterium Isolated from Nebraska's Eastern Saline Wetlands. Honors Theses, University of Nebraska-Lincoln, 2022, p. 450.

[44] E.v. Labelle, C.W. Marshall, H.D. May, Microbiome for the electrosynthesis of chemicals from carbon dioxide, Acc. Chem. Res. 53 (2020) 62−71, https://doi.org/10.1021/acs.accounts.9b00522.

[45] F. Asunis, G. de Gioannis, P. Dessì, M. Isipato, P.N.L. Lens, A. Muntoni, A. Polettini, R. Pomi, A. Rossi, D. Spiga, The dairy biorefinery: integrating treatment processes for cheese whey valorisation, J. Environ. Manag. 276 (2020), 111240, https://doi.org/10.1016/j.jenvman.2020.111240.

[46] Eurostat, Electricity prices for non-household consumers (2022) [WWW Document], https://ec.europa.eu/eurostat/statistics-explained/index.php?title=Electricity_price_statistics#Electricity_prices_for_non-household_consumers, 8.18.22.